MOBILITY MEASUREMENT BY ANALYSIS OF FLUORESCENCE PHOTOBLEACHING RECOVERY KINETICS

D. AXELROD, D. E. KOPPEL, J. SCHLESSINGER, E. ELSON, *and* W. W. WEBB

From the School of Applied and Engineering Physics, and Department of Chemistry, Cornell University, Ithaca, New York 14853

ABSTRACT Fluorescence photobleaching recovery (FPR) denotes a method for measuring two-dimensional lateral mobility of fluorescent particles, for example, the motion of fluorescently labeled molecules in $\sim 10\ \mu m^2$ regions of a single cell surface. A small spot on the fluorescent surface is photobleached by a brief exposure to an intense focused laser beam, and the subsequent recovery of the fluorescence is monitored by the same, but attenuated, laser beam. Recovery occurs by replenishment of intact fluorophore in the bleached spot by lateral transport from the surrounding surface. We present the theoretical basis and some practical guidelines for simple, rigorous analysis of FPR experiments. Information obtainable from FPR experiments includes: (*a*) identification of transport process type, i.e. the admixture of random diffusion and uniform directed flow; (*b*) determination of the absolute mobility coefficient, i.e. the diffusion constant and/or flow velocity; and (*c*) the fraction of total fluorophore which is mobile. To illustrate the experimental method and to verify the theory for diffusion, we describe some model experiments on aqueous solutions of rhodamine 6G.

INTRODUCTION

This paper describes experimental and theoretical aspects of a recently developed method, Fluorescence photobleaching recovery (FPR), for measuring transport of fluorescent molecules in small systems such as individual living cells. This work was prompted by our desire to measure rates of lateral transport of proteins and lipids in cell membranes. There is currently widespread interest in this problem because of the apparent role of lateral membrane transport as an indicator or effector of changes in the physiological states of cells (1–4). In addition to measurements of transport on membranes, FPR provides a broad capability for a variety of other applications.

The new method is simple both in concept and in practice. A small region of a surface containing mobile fluorescent molecules is exposed to a brief intense pulse of light (perhaps focused on the surface through the reflected illumination optics of a microscope), thereby causing irreversible photochemical bleaching of the fluorophore in that region. Transport coefficients (e.g. diffusion coefficients) are determined by measuring the rate of recovery of fluorescence which results from transport of fluorophore into the bleached region from unirradiated parts of the system. The fluorescence from the

bleached region is excited by a greatly attenuated beam in order to avoid significant photolysis during the recovery phase of the experiment. The fluorophore is photobleached at a wavelength which is not absorbed by and therefore does not destroy other components of the system (e.g., enzymes, coenzymes, or nucleic acids in a living cell).

Photobleaching techniques have been used by several researchers to study lateral transport of membrane proteins (5–10). Our version of the technique (10) employs a single, circularly symmetric, focused laser beam for both bleaching and, appropriately attenuated, for observation of recovery, so that mobility in $\sim 10\ \mu m^2$ regions can be examined. The analysis described here enables one to determine not only lateral transport rates, but also: (*a*) to distinguish between diffusion and systematic transport processes such as electrophoresis, convective flow, or other driven processes; and (*b*) to measure the ratio of mobile to immobile fluorophore on heterogeneous samples such as cell surfaces, where this ratio may be biologically significant. We further demonstrate the manner in which the shape of the fluorescence recovery curve depends not only upon beam profile, but on the amount of bleaching employed. Experimental data are presented which confirm the applicability of the theory to measurements of diffusion in a simple model system.

THEORETICAL RESULTS

We present here the theoretical fluorescence recovery curves for several idealized cases: (*a*) pure two-dimensional diffusion monitored by a laser beam of Gaussian intensity profile, and of uniform circular disc profile; (*b*) uniform flow across a Gaussian, and a uniform circular disc profile; and (*c*) simultaneous diffusion and flow across a Gaussian intensity profile. Although idealized, these cases are of practical importance because the laser beam intensity profile is commonly intermediate between Gaussian and uniform disc due to admixture of TEM 00 and TEM 01 modes.

For simplicity we require that photobleaching of the fluorophore to a nonfluorescent species is a simple irreversible first-order reaction with rate constant $\alpha I(r)$. Then the concentration of unbleached fluorophore, $C(r, t)$ at position r and time t in the absence of transport can be calculated from

$$\mathrm{d}C(r,t)/\mathrm{d}t = -\alpha I(r)\, C(r,t),$$

where $I(r)$ is the bleaching intensity. Hence, for a bleaching pulse which lasts a time interval T short compared with characteristic times for transport, the fluorophore concentration profile at the beginning of the recovery phase ($t = 0$) is given by

$$C(r,0) = C_o \exp\left[-\alpha T I(r)\right], \tag{1}$$

where C_o is the initial uniform fluorophore concentration.

The "amount" of bleaching induced in time T is expressed by a parameter K:

$$K \equiv \alpha T I(0). \tag{2}$$

For a Gaussian intensity profile, $I(r)$ is given by

$$I(r) = (2P_o/\pi w^2) \exp(-2r^2/w^2), \tag{3}$$

where w is the half-width at e^{-2} height, and P_o is the total laser power. Initial concentration profiles $C(r, 0)$ for a Gaussian beam at several bleach pulse energies are shown in Fig. 1.

For a circular disc profile, $I(r)$ is given by

$$I(r) = \begin{cases} P_o/\pi w^2 & r \leq w \\ 0 & r > w \end{cases} \tag{4}$$

where w here is the radius of the disc.

The differential equation for lateral transport of a single species of fluorophore by diffusion with diffusion coefficient D and uniform flow with velocity V_o in the x-direction is:

$$\partial C(r,t)/\partial t = D\nabla^2 C(r,t) - V_o[\partial C(r,t)/\partial x]. \tag{5}$$

The boundary condition is $C(\infty, t) = C_o$; the initial condition $C(r, 0)$ is given by Eq. 1.

The fluorescence $F_K(t)$ observed at time $t \geq 0$ is given by

$$F_K(t) \equiv (q/A) \int I(r) C_K(r,t) \mathrm{d}^2 r, \tag{6}$$

where $C_K(r, t)$ is the solution of Eq. 5 for the K-dependent initial condition given in Eq. 1; parameter q is the product of all the quantum efficiencies of light absorption, emission, and detection; and A is the attenuation factor of the beam during observa-

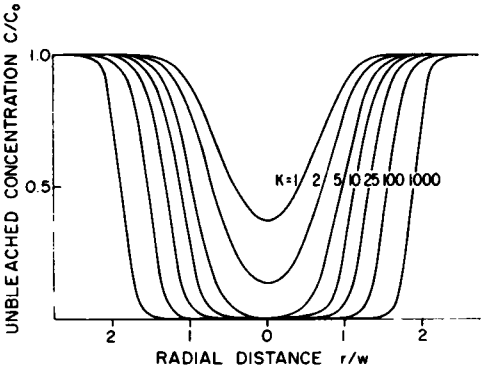

FIGURE 1 Normalized initial post-bleach fluorophore concentration $C(r, 0)/C_o$, with a Gaussian beam of radius w at e^{-2} intensity, for various values of the bleaching parameter K proportional to the bleach pulse energy.

tion of recovery. Before the beginning of bleaching, $F_K = qP_oC_o/A$. The initial fluorescence $F_K(0)$ after bleaching depends upon beam profile but not the mode of recovery:

$$F_K(0) = (qP_oC_o/A)K^{-1}(1 - e^{-K}), \tag{7}$$

for a Gaussian beam;

$$F_K(0) = (qP_oC_o/A)e^{-K}, \tag{8}$$

for a uniform circular disc. Eqs. 7 and 8 show how the K value of a recovery curve can be uniquely determined from its $t = 0$ point. A convenient way of displaying fluorescence recovery curves is in fractional form $f_K(t)$ defined as follows:

$$f_K(t) \equiv [F_K(t) - F_K(0)]/[F_K(\infty) - F_K(0)]. \tag{9}$$

In the following paragraphs only the essential results, solutions for $F_K(t)$ or $f_K(t)$, are presented; outlines of the derivations are displayed in the Appendix.

Diffusion ($V_o = 0$)

Gaussian Intensity Profile. The closed form solution is

$$F_K(t) = (qP_oC_o/A)\nu K^{-\nu}\Gamma(\nu)\,P(2K \mid 2\nu), \tag{10}$$

where $\nu \equiv (1 + 2t/\tau_D)^{-1}$; $\tau_D \equiv w^2/4D$, the "characteristic" diffusion time; and $\Gamma(\nu)$

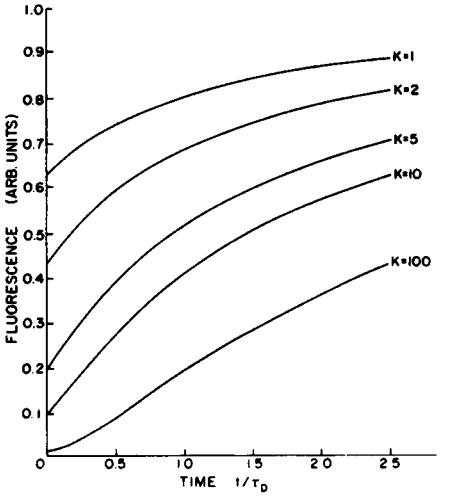

FIGURE 2

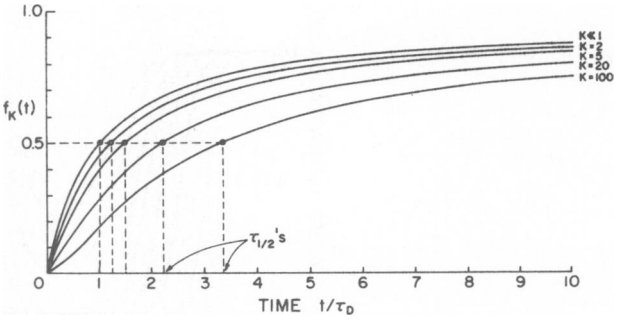

FIGURE 3

FIGURE 2 Normalized fluorescence recovery $F_K(t)$ vs. t/τ_D for diffusion, with Gaussian beam, for various values of K.

FIGURE 3 Fractional fluorescence recovery $f_K(t)$ vs. t/τ_D for diffusion, with a Gaussian beam, for various values of K. Note that the relationship between $\tau_{1/2}$ and τ_D depends upon K.

is the gamma function. The χ^2-probability distribution $P(2K \mid 2\nu)$ is tabulated in ref. 11 (p. 978). Fluorescence $F_K(t)$ and the related fractional fluorescence $f_K(t)$ are plotted in Figs. 2 and 3, respectively, as function of t/τ_D for various K values. For large K, where $P(2K \mid 2\nu)$ approaches one, Eq. 10 reduces to a simple approximate form:

$$F_K(t) \approx (qP_oC_o/A)\nu K^{-\nu}\Gamma(\nu), \tag{11}$$

to within 1% accuracy for $K \geq 4$ and $t/\tau_D \geq 0.25$.

A series solution for $F_K(t)$ valid for all K and t is:

$$F_K(t) = (qP_oC_o/A) \sum_{n=0}^{\infty} [(-K)^n/n!][1 + n(1 + 2t/\tau_D)]^{-1}. \tag{12}$$

For $K \ll 1$, this assumes the simple form

$$F_{K\ll 1}(t) = (qP_oC_o/A)[1 - K/2(1 + t/\tau_D)]. \tag{13}$$

Uniform Circle Profile. For this case, the fractional fluorescence recovery $f_K(t)$ is independent of the bleaching parameter K. A solution in the form of an integral over a P^* function (12) can be derived, but the following series solution is much more convenient for numerical evaluation:

$$f_K(t) = 1 - (\tau_D/t)\exp(-2\tau_D/t)[\mathbf{I}_o(2\tau_D/t) + \mathbf{I}_2(2\tau_D/t)] + 2\sum_{k=0}^{\infty} \frac{(-1)^k(2k + 2)!(k + 1)!(\tau_D/t)^{k+2}}{(k!)^2[(k + 2)!]^2}, \tag{14}$$

where $\mathbf{I}_o$ and $\mathbf{I}_2$ are modified Bessel functions and $\tau_D = w^2/4D$. In Fig. 4 we plot $f_K(t)$ vs. t/τ_D.

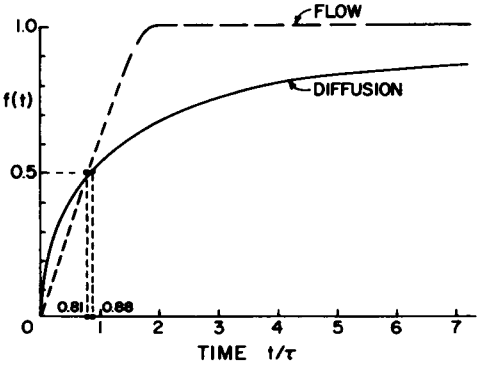

FIGURE 4 Fractional fluorescence recovery $f_K(t)$ vs. t/τ for diffusion (—) and for flow (- - -), with a uniform circular disc beam.

Uniform Flow ($D = 0$)

Gaussian Profile. The fluorescence $F_K(t)$ is given by

$$F_K(t) = (qP_oC_o/A)\pi^{-1}\int\rho d\rho d\theta \exp[-K\exp(-\rho^2) - \rho'^2], \quad (15)$$

where $\rho'^2 \equiv \rho^2 + 2(t/\tau_F)^2 - 8^{1/2}(t/\tau_F)\rho\cos\theta$ and $\tau_F \equiv w/V_o$. We have calculated the integral of Eq. 15 numerically by computer for various K values. The fractional fluorescence recovery $f_K(t)$ as a function of t/τ_F for various K values is plotted in Fig. 5.

A series solution for this case is

$$F_K(t) = (qP_oC_o/A)\sum_{n=0}^{\infty}(-K)^n/(n+1)!\exp\{[-2n/(n+1)](t/\tau_F)^2\} \quad (16)$$

Uniform Circle Profile. This case has a simple analytical solution derived by calculating the area of non-overlap of two circles of radius a whose centers are displaced by x. The fractional fluorescence recovery $f_K(t)$ is

$$f_K(t) = (2/\pi)\sin^{-1}(t/2\tau_F) + (t/\tau_F)(1 - t^2/4\tau_f^2)^{1/2}, \quad (17)$$

where $\tau_V \equiv w/V_o$ and $t \leq 2\tau_F$. This function is plotted in Fig. 4; again $f_K(t)$ is independent of K as expected.

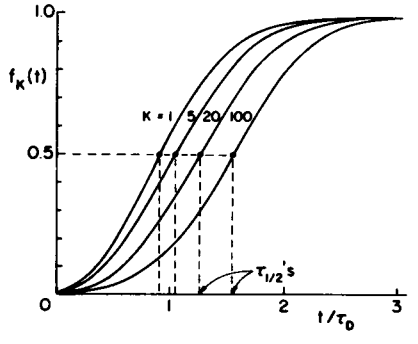

FIGURE 5

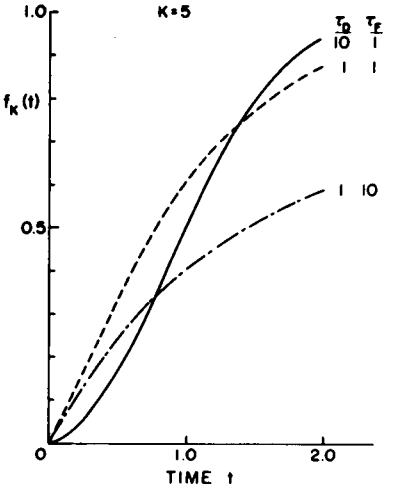

FIGURE 6

FIGURE 5 Fractional fluorescence recovery $f_K(t)$ vs. t/τ_D for flow, with a Gaussian beam, for various values of K.

FIGURE 6 Fractional fluorescence recovery $f_K(t)$ vs. t (arbitrary units) for combined flow and diffusion with a Gaussian beam and $K = 5$, for values of (τ_D, τ_F) equal to (10, 1) (——); (1, 1) (- - -); and (1, 10) (— - —).

Combined Flow and Diffusion: Gaussian Profile. The series solution for $F_K(t)$ is

$$F_K(t) = (qP_oC_o/A)\sum_{n=0}^{\infty} \frac{(-K)^n \exp\{-2(t/\tau_F)^2 n/[1 + n(1 + 2t/\tau_D)]\}}{n![1 + n(1 + 2t/\tau_D)]}. \quad (18)$$

The fractional fluorescence $f_K(t)$ vs. t is plotted in Fig. 6 for $K = 5$ and $\tau_F/\tau_D = 10$, 1, and 0.1.

Analysis of experimental data using these equation is discussed in the next section.

EXPERIMENTAL DATA ANALYSIS

The goals of fitting experimental data to our theoretical results are to determine: (*a*) the nature of the transport (i.e., flow, diffusion, or a combination of the two); (*b*) the relative proportion of mobile vs. immobile fluorophore in the sample (which may be of considerable interest in mobility measurements on living cells); and (*c*) the apparent diffusion constant D or flow rate V_o. Absolute determination of D and V_o depends upon determinations of beam size and profile; we discuss the calibration problem immediately after the curve fitting problem.

Curve Fitting

We have developed two simplified procedures for routine analyses. Let $\hat{F}_K(t)$ and $\hat{f}_K(t)$ represent an experimental recovery curve in arbitrary units and in fractional form, respectively. We define $\hat{F}_K(-)$ to be the fluorescence before bleaching.

The first approach, essentially a three-point fit of the data, is especially useful when the nature of transport and $\hat{F}_K(\infty)$ are known. One proceeds as follows:

(*i*) Determine the time $\tau_{1/2}$ for which $\hat{f}_K(\tau_{1/2}) = 1/2$;

(*ii*) If the beam is Gaussian, determine $\hat{F}_K(0)/\hat{F}_K(-)$ and use Eq. 7 to calculate the bleaching parameter K;

(*iii*) Calculate the mobility rate by one of the following formulas:

$$\text{Diffusion:} \quad D = (w^2/4\tau_{1/2})\gamma_D, \quad (19)$$

$$\text{Flow:} \quad V_o = (w/\tau_{1/2})\gamma_F. \quad (20)$$

Constants γ_D and γ_F are given by $\gamma_D \equiv \tau_{1/2}/\tau_D$ and $\gamma_F \equiv \tau_{1/2}/\tau_F$, respectively. In general, γ_D and γ_F depend upon beam shape, type of transport and K. Fig. 7 shows γ_D and γ_F vs. K for Gaussian beam diffusion and flow, respectively. For circular beams, $\gamma_D = 0.88$ and $\gamma_F = 0.81$, independent of K.

If some of the fluorophore in the illuminated region is immobile, the asymptote of the fluorescence recovery after bleaching, $\hat{F}_K(\infty)$, will be less than $\hat{F}_K(-)$. The fraction of total fluorophore which is mobile is given by

$$[\hat{F}_K(\infty) - \hat{F}_K(0)]/[\hat{F}_K(-) - \hat{F}_K(0)].$$

The second approach to data analysis is based upon the observation that plots of $[F_K(t) - F_K(0)]$ vs. t and $f_K(t)$ vs. t/τ are different, in general, by two multiplicative

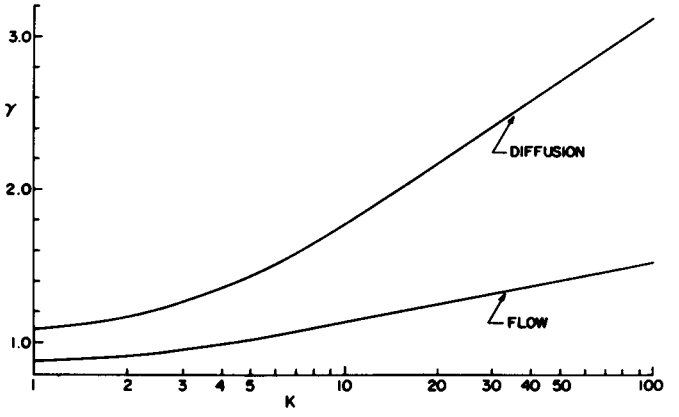

FIGURE 7 Factor γ, (γ_D or γ_F), vs. K for a Gaussian beam.

factors: a vertical scale factor and a time scale factor. In log-log plots these multiplicative factors are transformed to orthogonal displacements along the vertical and time axes. It is thus possible to determine the vertical and time factors from the size of the orthogonal displacements needed for optimal superposition of log-log plots of $[\hat{F}(t) - \hat{F}(0)]$ vs. t and the appropriate theoretical $f_K(t)$ vs. t/τ. These scale factors completely characterize the fit to the theory, giving both the percent recovery and the characteristic time. In this fitting approach, therefore, it is unnecessary to estimate directly the long-time asymptote of fluorescence recovery $F_K(\infty)$. Fig. 9 graphically illustrates the log-log superposition of $f_K(t)$ with experimentally obtained data.

In order to determine whether the recovery curve represents diffusion, flow, a combination of the two, or some other type of transport, log-log plots of experimental $[\hat{F}_K(t) - \hat{F}_K(0)]$ should be matched with trial theoretical $f_K(t/\tau)$ curves. However, some information can be extracted from certain salient features of the experimental curve without invoking the log-log superposition procedure. For the Gaussian beam case, flow recovery always shows a "sigmoidal" (i.e., containing an inflection point) shape, whereas diffusional recovery curves are sigmoidal only at very high K. Note, however, that a mixture of diffusion and flow may not show a sigmoidal shape recovery. For the circular disc beam case, neither flow nor diffusional recovery shows a sigmoidal shape. However, only for pure flow does the fluorescence reach its recovery limit in a finite time, although this distinction may not be apparent except in precise data.

The characteristic time for flow recovery is proportional to w; the characteristic time for diffusional recovery is proportional to w^2. Thus, observing how the time axis of the recovery scales with beam size provides a powerful means of distinguishing flow from diffusional motion. For mixtures of the two, small w tends to make diffusion dominant in determining recovery curve shape; large w makes flow dominant.

If the sample is composed of more than one independent diffusing species of different mobilities, the $\tau_{1/2}$ of the recovery curve still scales with w^2 (if K is kept constant) but the slope of the curve at early times is abnormally high, relative to late times. As a re-

sult, multiple independent diffusion should be distinquishable from single diffusion mixed with flow. If the diffusion constants of the mixture are well separated, log-log plot superpositions preferentially matched at early and late times yield the characteristic time of the fastest and slowest diffusion, respectively.

Absolute Calibration

To determine transport coefficients absolutely, it is necessary to characterize the size and shape of the focused laser beam profile. Many experimental approaches to this characterization involve the translation of a specimen through the beam at a known constant velocity. One can analyze the signal from a thin dilute layer of fluorescing or scattering particles, or monitor the trace of fluorescence from a spider web strand or the intensity of light reflected or transmitted by a knife edge. For a known or assumed beam shape, each of the above approaches gives an accurate determination of beam size. They give only an integral over the beam profile, however, and are therefore not very sensitive to details of the beam shape.

Perhaps the best way of characterizing the laser beam profile is to use the FPR technique itself, i.e., to scan with known velocity through a spot bleached in a thin layer of immobile fluorophore. Such a calibration scan, performed with the same bleaching parameter K as the experiment, generates a "flow" recovery curve which clearly can be used to calibrate a flow experiment for arbitrary beam size and shape. It has, however, remarkable and unexpected advantages for calibrating a diffusion determination as well. Combining Eq. 19 and 20, we have for our determination of D:

$$D = (V_o^2 \gamma_D / 4\gamma_F^2)[(\tau_{1/2}^C)^2/\tau_{1/2}], \tag{21}$$

where V_o is the known velocity of the calibration scan, and $\tau_{1/2}$ and $\tau_{1/2}^C$ are the 50% recovery times for the diffusion experiment and the calibration scan, respectively. The factors γ_D and γ_F are, in general, functions of both the beam shape and the extent of bleaching (see Fig. 7). It is an empirical fact, however, that the combination γ_D/γ_F^2 has, for all practical purposes, a single value for both a uniform circle beam and a Gaussian beam for K values at least up to 100. Under these conditions, to within better than 4%:

$$D = 0.35\, V_o^2(\tau_{1/2}^C)^2/\tau_{1/2}. \tag{22}$$

It remains to be seen whether or not this relation holds for other beam profiles as well.

EXPERIMENTAL TESTS WITH A MODEL SYSTEM

The application of FPR to diffusional recovery for a nominally Gaussian beam was tested experimentally on a thin aqueous layer of rhodamine 6G in either H_2O or 1:1 (vol) glycerol:H_2O at 25°C.

Methods

The optical and electronic system is illustrated in Fig. 8. The laser beam was attenuated by a factor of 10^4 between bleaching and fluorescence observation; this factor

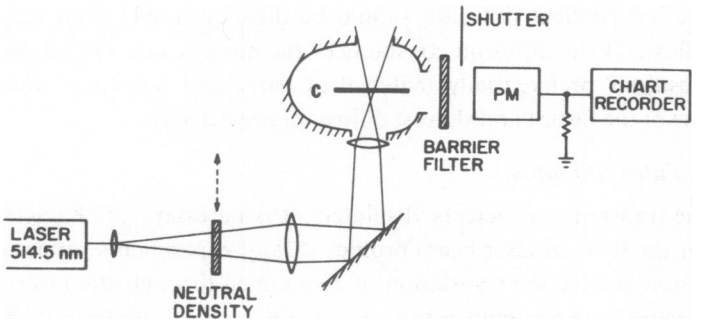

FIGURE 8 Optics and electronics of the model system test. Bleaching laser (Spectra-Physics, Mountain View, Calif., model 164) power was 1 W. The rhodamine 6G (Fisher Scientific Co., Pittsburgh, Pa.) aqueous solution concentration for all experiments was 4.6×10^{-6}M, contained in a rectangular Suprasil quartz cuvette (C) of 100 μm path length. The photomultiplier (PM) was an EMI 9658 R. The barrier filter was saturated aqueous potassium dichromate solution.

assures that the amount of fluorophore bleached during the observation period will be no more than 1% of that bleached initially. Bleaching time T was always less than 10% of τ_D. The beam profile was obtained by measuring the laser light transmitted past a razor blade edge as it translates across the beam at the sample position; spot size was varied by vertical adjustment of the focusing beam lens relative to the sample position.

The fluorescence decay of R6G in H_2O and 1:1 glycerol:H_2O in a closed uniformly illuminated volume was measured and confirmed to be approximately exponential with only a negligible amount of dark recovery. This test is important because the theoretical treatment presented here is not applicable if significant chemical recovery of fluorescence occurs in the time scale of the experiment or if the bleaching reaction is complex. Since reversibility of photobleaching is common and depends upon solvent effects, impurities, and local environment of the fluorophore, it must be checked under the conditions of the intended experiment. For example, in experiments in single living cells an entire cell should be uniformly bleached so that possible fluorescence recovery due to chemical reversibility can be observed in the absence of recovery due to transport.

Results

Table I shows the computed D values of several runs of various K, w, and published viscosity values. The average diffusion constant D for R6G in H_2O is $(1.2 \pm 0.2) \times 10^{-6}$ cm^2/s; in 1:1 (vol) glycerol-H_2O, D is $(0.26 \pm 0.09) \times 10^{-6}$ cm^2/s. The uncertainties are based upon reproducibility. The ratio of the two is approximately equal to the ratio of viscosities of the two solvents, as expected. The scaling of τ_D with w^2 is correct to within the uncertainty; there is no apparent systematic dependence on K.

The data was fit to the theory by the log-log method since recovery was usually less than 100% complete due to dye adhering to the glass surfaces. Fig. 9 shows the match of theory to experiment for a typical run. The fit is very close, but there is a consistent

TABLE I

Solvent viscosity	K	w	D
cp		μm	$\times 10^{-6}\ cm^2/s$
1	1.40	153	1.24
1	1.89	153	1.43
1	2.29	153	1.17
1	1.91	102	0.96
1	1.63	204	1.30
4.5	1.86	102	0.19
4.5	0.79	153	0.32

difference apparent at early times. We believe this slight discrepancy is due to the measured slightly non-Gaussian contour of the beam profile. The nonideality of the beam profile leads to an ambiguity in our measurements of w of about $\pm 15\%$ and a consequent uncertainty in D of $\pm 30\%$. This type of uncertainty in D could be substantially reduced in principal with the calibration procedure described above. Relative transport rates at different times or in different regions in the same sample can be determined more accurately since they are not affected by uncertainties in w.

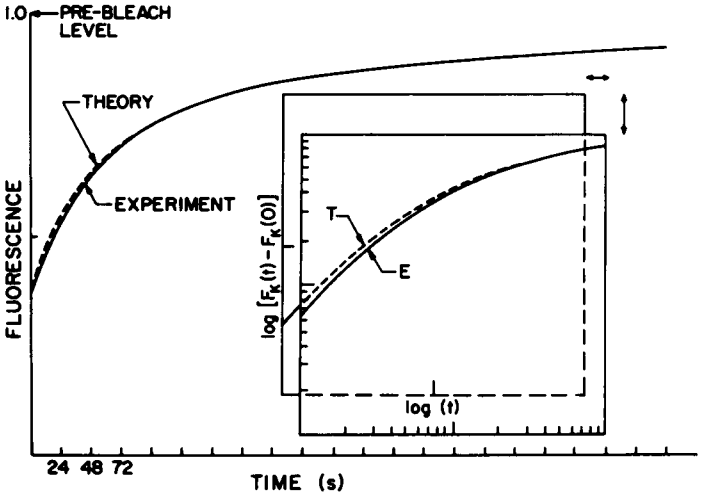

FIGURE 9 A graphic illustration of the log-log superposition method for a "best fit" of theoretical curves to experimental data. The resulting superposition of the $t/\tau = 1$ point on the time axis of the theoretical plot of $\log f_K(t)$ vs. t/τ with the time axis of the experimental plot of $\log [\hat{F}_K(t) - \hat{F}_K(0)]$ gives the experimental characteristic time τ. Likewise, superposition of the $f_K(t) = 1$ point on the ordinate of the theoretical plot with the ordinate of the experimental plot gives $\hat{F}_K(\infty) - \hat{F}_K(0)$, from which the mobile fraction $[\hat{F}_K(\infty) - \hat{F}_K(0)]/[\hat{F}_K(-) - \hat{F}_K(0)]$ can be calculated. This method was applied to the model system fluorescence recovery data and both the experimental curve (——) and the theoretical fit (- - -) were replotted on a linear fluorescence vs. t scale. The particular run illustrated here is 4.6×10^{-6}M rhodamine 6G in H_2O at 22°C with $w = 153\ \mu m$ and $K = 2.29$. The characteristic time τ is 50 s, the mobile fraction is 0.95, and the computed diffusion constant D is $1.17 \times 10^{-6}\ cm^2/s$. Laser bleaching power is 1 W; bleaching duration is 1 s.

K was confirmed to increase approximately linearly with bleaching time T in the range of T values used. If proportionality of K with T and I_o is not experimentally upheld, then at least one of the assumptions of the theory is being violated. If local heating induces mass transport in the sample, or if T is not much less than τ, the apparent K will increase too slowly with I_o or T, respectively, and τ will be overestimated. Deviation of the beam profile from its expected shape also may remove the strict proportionality of K with I_o and T.

DISCUSSION

We have demonstrated that observation of fluorescence photo-bleaching recovery kinetics can be analyzed to determine lateral mobility rates, to distinguish between flow and diffusional transport, and to determine the fraction of the total fluorophore which is immobile. In a separate communication (17), the features of FPR are compared in detail with those of another microfluorimetric technique, fluoroescence correlation spectroscopy (13–16) which also directly measures lateral mobility.

A wide range of mobility rates can be measured by FPR. The maximum measurable mobility rate may be limited by available bleaching power. For a 1 W laser output, a dye of extinction coefficient $\epsilon = 10^5$ liters/mol·cm and $T \leq \tau/10$, a fluorophore with a diffusion constant of $D \leq 10q_B$ (q_B is photobleaching quantum efficiency) can be bleached with $K \gtrsim 1$. The value of K actually needed for a given experiment depends upon the level of shot noise and systematic fluctuations. For a small w, the maximum measurable transport rate may also be limited by the speed of the excitation and emission beam shutters. The experimental verification with a thin aqueous R6G layer demonstrates that the method works to diffusion constants at least as fast as 10^{-6} cm^2/s.

At the other extreme of mobility, successful measurements of lateral mobility of labeled proteins on tissue culture cells (10) through specially adapted microscope optics (17) were sensitive to lateral transport rates equivalent to diffusion constants as low as 10^{-11} cm^2/s. The minimum diffusion rate measurable is limited only by the DC stability of the electronics or sample. Operating between these extremes, the technique should be highly useful in measuring lateral motions of fluorescent macromolecules in solution, in lipid bilayers, and on cell surfaces.

We thank Mr. Richard Cochran for writing the computer program used in this study and Ms. B. Meger for typing the manuscript.

We are pleased to acknowledge the support of NIH grant no. GM-21661, the National Science Foundation Division of Condensed Matter, a European Molecular Biology Organization travel grant (J. Schlessinger), an NIH Postdoctoral Fellowship NS-00432A (D. Axelrod), an NIH Career Development Award (E. Elson), a Guggenheim Fellowship (W. W. Webb), and a grant from the Research Corporation.

Received for publication 14 April 1976.

REFERENCES

1. EDIDIN, M. 1974. Rotational and translational diffusion in membranes. *Ann. Rev. Biophys. Bioeng.* 3:179.

2. BRETSCHER, M. S., and M. C. RAFF. 1975. Mammalian plasma membranes. *Nature (Lond.).* **258**:43.
3. EDELMAN, G. M. 1974. Surface alterations and mitogenesis in lymphocytes. *In* Control of Proliferation in Animal Cells. B. Clarkson and R. Baserga, editors. Cold Spring Harbor Laboratory of Quantitative Biology, Cold Spring Harbor, N.Y. 357.
4. YAHARA, I., and G. M. EDELMAN. 1972. Restriction of the mobility of lymphocyte immunoglobulin receptors by concanavalin A. *Proc. Natl. Acad. Sci. U.S.A.* **69**:608.
5. POO, M.-M., and R. A. CONE. 1974. Lateral diffusion of rhodopsin in the photoreceptor membrane. *Nature (Lond.).* **247**:438.
6. PETERS, R., J. PETERS, K. H. TEWS, and W. BÄHR. 1974. A microfluorimetric study of translational diffusion in erythrocyte membranes. *Biochim. Biophys. Acta.* **367**:282.
7. EDIDIN, M., Y. ZAGYANSKY, and T. J. LARDNER.1976. Measurement of membrane protein lateral diffusion in single cells. *Science (Wash. D.C.).* **191**:466.
8. ZAGYANSKY, Y., and M. EDIDIN. 1976. Lateral diffusion of concanavalin A receptors in the plasma membrane of mouse fibroblasts. *Biochim. Biophys. Acta.* **433**:209.
9. JACOBSON, K., E. WU, and G. POSTE. 1976. Measurement of the translational mobility of Concanavalin A in glycerol-saline solutions and on the cell surface by fluorescence recovery after photobleaching. *Biochim. Biophys. Acta.* **433**:215.
10. SCHLESSINGER, J., D. E. KOPPEL, D. AXELROD, K. JACOBSON, W. W. WEBB, and E. L. ELSON. 1976. Lateral mobility on cell membranes: the mobility of concanavalin A receptors on myoblasts. *Proc. Natl. Acad. Sci. U.S.A.* **73**(7). In press.
11. ABRAMOWITZ, M., and I. A. STEGUN, eds. 1965. Handbook of Mathematical Functions. Dover Publications, Inc., New York.
12. MASTERS, J. I. 1954. Some applications in physics of the P function. *J. Chem. Phys.* **23**:1865.
13. ELSON, E. L., and D. MAGDE. 1974. Fluorescence correlation spectroscopy. I. Conceptual basis and theory. *Biopolymers.* **13**:1.
14. MAGDE, D., E. L. ELSON, and W. W. WEBB. 1974. Fluorescence correlation spectroscopy. II. An experimental realization. *Biopolymers.* **13**:29.
15. KOPPEL, D. E. 1974. Statistical accuracy in fluorescence correlation spectroscopy. *Phys. Rev. A.* **10**:1938.
16. ELSON, E. L., and W. W. WEBB. 1975. Concentration correlation spectroscopy: a new biophysical probe based on occupation number fluctuations. *Ann. Rev. Biophys. Bioeng.* **4**:311.
17. KOPPEL, D. E., D. AXELROD, J. SCHLESSINGER, E. L. ELSON, and W. W. WEBB. 1976. Dynamics of fluorescence marker concentration as a probe of mobility. *Biophys. J.* **16** (2, pt. 2):216*a*. (Abstr.). (Manuscript submitted to *Biophys. J.* for publication.)
18. CARSLAW, H. S., and J. C. JAEGER. 1947. Conduction of Heat in Solids. Oxford University Press, London.

APPENDIX

We present here outlines of the derivations of the theoretical fluorescence recovery curves. The methods to obtain the series solutions and the closed form or integral solutions differ, so they will be discussed separately.

Series Solutions

Eq. 5 is solved by Fourier transformation subject to the previously stated boundary and initial conditions. The approach is similar to that of ref. 13, which may be consulted for a detailed discussion of an analogous, although more complex, problem.

Fourier transformation of Eq. 5 yields

$$d\tilde{C}(\mu, t)/dt = -[\mu^2 D - i\mu_x V_o]\tilde{C}(\mu, t), \tag{23}$$

where $\mu^2 = \mu_x^2 + \mu_y^2$. The solution of Eq. 23 is

$$\tilde{C}(\mu, t) = \tilde{C}(\mu, 0) \exp[-(\mu^2 D - iV_o\mu_x)t].$$

Since $\tilde{C}(\mu, 0) = (2\pi)^{-1} \int d^2 r e^{i\mu \cdot r} C(r, 0)$ with $C(r, 0)$ given by Eq. 1 and

$$C(r, t) = (2\pi)^{-1} \int e^{-i\mu \cdot r} \tilde{C}(\mu, t) d^2\mu,$$

we obtain from Eq. 6

$$F_K(t) = (qC_o/4\pi^2 A) \int d^2\mu \phi(\mu) e^{-[\mu^2 D - iV_o \mu_x]t}, \tag{24}$$

where

$$\phi(\mu) \equiv \int d^2 r I(r) \exp[-i\mu \cdot r] \int d^2 r' \exp[i\mu \cdot \mathbf{r}' - \alpha I(r') T] \tag{25}$$

is a function which depends on the laser intensity profile but not on the mechanism of transport. Eq. 24 may be used for pure diffusion or pure flow by setting $V_o = 0$ or $D = 0$, respectively.

Gaussian Beam: Diffusion and Flow. The series solutions for the Gaussian beam intensity profile are developed by expanding $\exp[-\alpha I(r') T]$ and performing the integrations explicitly for a general term in the series.

Circular Disc Beam: Diffusion. Substituting the circular disc profile into Eq. 25 and using standard identities yields

$$\phi(\mu) = I_o\{8\pi^3 w[\mathbf{J}_1(w\mu)/\mu]\delta(\mu) - (1 - e^{-K})(2\pi w)^2[\mathbf{J}_1(w\mu)/\mu]^2\}. \tag{26}$$

Substitution of this result into Eq. 24 yields

$$F(t) = (qP_o C_o/A)\left\{1 - 2(1 - e^{-K}) \int_0^\infty [\mathbf{J}_1(w\mu)/\mu]^2 e^{-\mu^2 Dt} \mu d\mu\right\}.$$

From this point, following the approach used in Appendix 2 of ref. 13 to reduce a similar integral, we arrive at Eq. 14.

Closed Form Diffusion Solution: Gaussian Beam

The starting equation for this approach is the solution of the diffusion equation in integral form (18):

$$C_K(r, t) = \exp(-r^2/4DT)/2Dt$$

$$\cdot \int_0^\infty \exp(-r'^2/4Dt) \mathbf{I}_o(rr'/2Dt) C_K(r', 0) r' dr', \tag{27}$$

where $\mathbf{I}_o$ is a modified Bessel function.

We substitute the initial post-bleach fluorophore concentration $C_K(r'0)$, given by Eqs. 1 and 3, into Eq. 27 and then use Eq. 6 to express the observed fluorescence recovery $F_K(t)$ as a double integral over r- and r'-space.

The r-integration should be performed first, noting that ordinary Bessel function $\mathbf{J}_o(iz) = \mathbf{I}_o(z)$ and (see ref. 11, p. 468)

$$\int_0^\infty \exp(-a^2 r^2) \mathbf{J}_o(br) r dr = \exp(-b^2/4a^2)/2a^2.$$

The r' integration can be performed by making the substitution $u \equiv K \exp(-2r'^2/w^2)$. Eq. 6 then becomes

$$F_K(t) = (qP_oC_o/A)\nu K^{-\nu} \int_0^K u^{\nu-1} e^{-u}\, du, \tag{27}$$

where ν is defined following Eq. 10. The integral is equal to the product of the gamma function $\Gamma(\nu)$ and the χ^2-probability distribution $P(2K \mid 2\nu)$, leading to the result, Eq. 10.

The simple exact expression for $F_K(0)$, Eq. 7, can be derived by calculating $\int I(r) C_K(r, 0) d^2r$ directly.